# Facet-Dependent Catalytic Activity of Cu₂O Nanocrystals in the One-Pot Synthesis of 1,2,3-Triazoles by Multicomponent Click Reactions

## Kaushik Chanda, Sourav Rej, and Michael H. Huang*[a]

**Abstract:** We report the highly facet-dependent catalytic activity of Cu₂O nanocubes, octahedra, and rhombic dodecahedra for the multicomponent direct synthesis of 1,2,3-triazoles from the reaction of alkynes, organic halides, and NaN₃. The catalytic activities of clean surfactant-removed Cu₂O nanocrystals with the same total surface area were compared. Rhombic dodecahedral Cu₂O nanocrystals bounded by {110} facets were much more catalytically active than Cu₂O octahedra exposing {111} facets, whereas Cu₂O nanocubes displayed the slowest catalytic activity. The superior catalytic activity of Cu₂O rhombic dodecahedra is attributed to the fully exposed surface Cu atoms on the {110} facet. A large series of 1,4-disubstituted 1,2,3-triazoles have been synthesized in excellent yields with high regioselectivity under green conditions by using these rhombic dodecahedral Cu₂O catalysts, including the synthesis of rufinamide, an antiepileptic drug, demonstrating the potential of these nanocrystals as promising heterogeneous catalysts for other important coupling reactions.

**Keywords:** click chemistry · copper · multicomponent reactions · nanocrystals · synthetic methods

## Introduction

The recent development in the syntheses of cuprous oxide (Cu₂O) and silver oxide (Ag₂O) nanocrystals in aqueous solutions with systematic shape evolution has yielded sharp-faced oxide nanocubes, octahedra, and rhombic dodecahedra bounded exclusively by the {100}, {111}, and {110} surfaces, respectively.[1–6] Their facet-dependent photocatalytic, electrical, and molecular adsorption properties can be investigated with greater certainty.[2,3,5–11] The relative stability of these surface planes toward face-selective chemical etching has been studied using particles exposing two or more of these surface facets.[12,13] Comparative catalytic activity of these nanostructures represents another important surface-related property to study. Examinations of facet-dependent cross-coupling reactions catalyzed by Cu₂O and other oxide nanocrystals exposing these low-index facets are highly interesting and attractive, but such studies are not quite possible due to the availability of rhombic dodecahedra until recently. Bulky Cu₂O and nanoparticles have been reported to be efficient catalysts for C−C and C−O bond-formation reactions.[14] Cu₂O nanocubes, rhombic dodecahedra, and octadecahedra were used for the aerobic oxidative arylation of arylboronic acid and phenylacetylene.[15] Cu₂O nanocubes, octahedra, nanospheres, and etched nanocubes can catalyze the N-arylation of imidazole with iodobenzene.[16] A reaction time of 10–15 h at 110 °C was found to be generally necessary to reach a product yield of more than 90 %. Since the pioneering work by Sharpless[17] and co-workers in 2001, the copper(I)- catalyzed 1,3-dipolar cycloaddition reaction[18] of organic azides and terminal alkynes also known as "click" chemistry has a powerful impact on drug discovery, organic synthesis, and biological and electrochemical applications.[19] The most practical aspect of click chemistry is the ability to attach diverse structures with a wide range of functional groups. Click reactions generating a diverse array of 1,2,3-triazoles represent highly desirable reactions that may be catalyzed by Cu₂O nanocrystals, since the Cu^I state has been known to be active for click reactions. Copper nanoparticles have been reported to catalyze cycloaddition of azides with terminal alkynes.[20] A click reaction performed on a Cu(111) surface under ultrahigh vacuum conditions was also demonstrated.[21] Recently, irregularly-shaped and polyvinylpyrrolidone (PVP)-coated Cu₂O nanoparticles were used to catalyze cycloaddition reactions between azides and alkynes in water under aerobic conditions.[22] A reaction time of 24 h at 37 °C was needed to reach product yields of 68–92 % for a range of azides and alkynes examined. Clearly the use of polyhedral Cu₂O nanocrystals as efficient catalysts for click reactions is essentially not studied. Facet-dependent catalytic activity of Cu₂O nanocrystals for the triazole-forming cycloaddition reactions remains unexplored.

In this study, we have used sharp-faced Cu₂O nanocubes, octahedra, and rhombic dodecahedra synthesized in aqueous solutions as catalysts for a range of Huisgen [3+2] cycloaddition reactions, or 1,3-dipolar cycloaddition, to examine the

[a] Dr. K. Chanda,⁺ S. Rej,⁺ Prof. Dr. M. H. Huang
Department of Chemistry and Frontier Research Center
on Fundamental and Applied Sciences of Matters
National Tsing Hua University, Hsinchu 30013 (Taiwan)
E-mail: hyhuang@mx.nthu.edu.tw

[⁺] These authors contributed equally to this work.

⌨ Supporting information for this article is available on the WWW under http://dx.doi.org/10.1002/chem.201302065.

facet-dependent catalytic activity of these $Cu_2O$ nanocrystals for the first time. Nanocrystals with approximately the same total surface area were employed to precisely compare the catalytic activity of different surface planes. Crystal models of the different planes of $Cu_2O$ and zeta potential measurements of the nanocrystals were used to explain the high catalytic activity of rhombic dodecahedra. Rhombic dodecahedra are highly efficient at coupling alkynes and organic halides in the presence of $NaN_3$ to generate diversely 1,4-disubstituted 1,2,3-triazoles in excellent yields with high regioselectivity under green conditions. Remarkably, the multicomponent coupling strategy can be easily extended to the synthesis of rufinamide (**A**), an antiepileptic drug, demonstrating the potential of $Cu_2O$ rhombic dodecahedra for applications in the synthesis of pharmaceutically active compounds.

## Results and Discussion

The $Cu_2O$ nanocubes, octahedra, and rhombic dodecahedra were synthesized in aqueous solutions following our previously reported procedures.[2,3] Precise amounts of $CuCl_2$ solution, SDS surfactant, NaOH solution, and $NH_2OH \cdot HCl$ reductant were mixed at room temperature and aged for 1–2 h for particle growth. Figure 1 shows the SEM images of the $Cu_2O$ nanocubes, octahedra, and rhombic dodecahedra synthesized with sizes of a few hundreds of nanometers. Rhombic dodecahedra are more uniformly-sized, whereas octahedra and cubes have larger size distributions. All nanocrystals possess sharp faces for their facet-dependent catalytic activity investigation. Figure S1 in the Supporting Information shows the higher-magnification SEM images of the nanocrystals and photographs of the particle solutions. Their size distribution histograms and the average particle sizes are given in Figure S2 and Table S1 (the Supporting Information). The solutions change from orange for the rhombic dodecahedra to dark-brown for the octahedra as the particle size increases. X-ray diffraction (XRD) patterns of these nanocrystals match to that of $Cu_2O$ (Figure S3, the Supporting Information). Rhombic dodecahedra showed enhanced (110) and (220) peaks as a result of their {110} faces. Octahdra displayed an exceptionally strong (111) reflection peak and very weak intensities for the other peaks possibly because most of the octahedra were oriented with their {111} faces parallel to the substrate plane. The cubes were more randomly oriented, so the relative peak intensities resemble those in the standard XRD pattern of $Cu_2O$.

For catalytic activity comparison of different surface facets, it is most desirable that capping surfactant is cleanly removed from the surfaces of the nanocrystals. After synthesis, the nanocrystals were washed with ethanol to remove the sodium dodecyl sulfate (SDS) surfactant completely. To confirm that the nanocrystal surfaces were clean and free from SDS or any kind of adsorbed organic molecules, Fourier transform infrared spectroscopy (FTIR) measurements were carried out on these nanocrystals (Figure S4, the Sup-
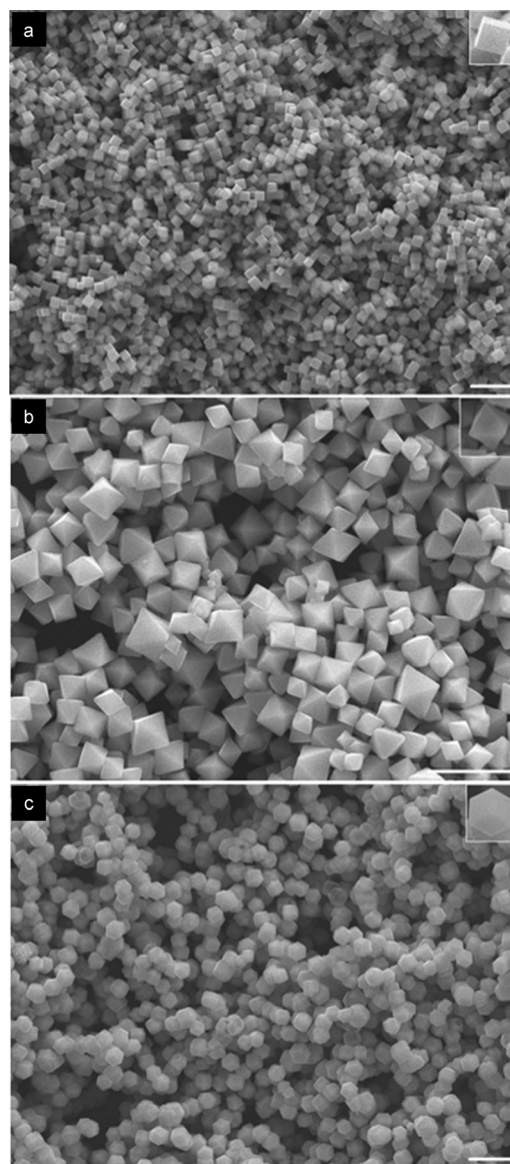


Figure 1. SEM images of a) cubic, b) octahedral, and c) rhombic dodecahedral $Cu_2O$ nanocrystals synthesized. Magnified SEM images of the different particle shapes are also provided. The scale bars are equal to 1 μm.

porting Information). Essentially, only two bands were observed in their FTIR spectra. The sharp peak at 631 cm$^{-1}$ corresponds to the Cu–O lattice vibration.[23] The band at around 3440 cm$^{-1}$ is attributed to the –OH stretching vibration, which comes from the surface-adsorbed $H_2O$. The absence of stretching frequency for C–H bonds, which generally appears in the range of 2850–2960 cm$^{-1}$, proves that the surfaces were free from surfactant. X-ray photoelectron spectrum (XPS) of the $Cu_2O$ rhombic dodecahedra provides further evidence for the absence of SDS from the particle surfaces (Figure 2). First, oxidation state of Cu in the particles was analyzed. In the Cu2p region, peaks at 932.1 and 951.9 eV are identified as the Cu2p$_{3/2}$ and Cu2p$_{1/2}$ characteristic peaks, respectively.[24] These peak positions are consis-
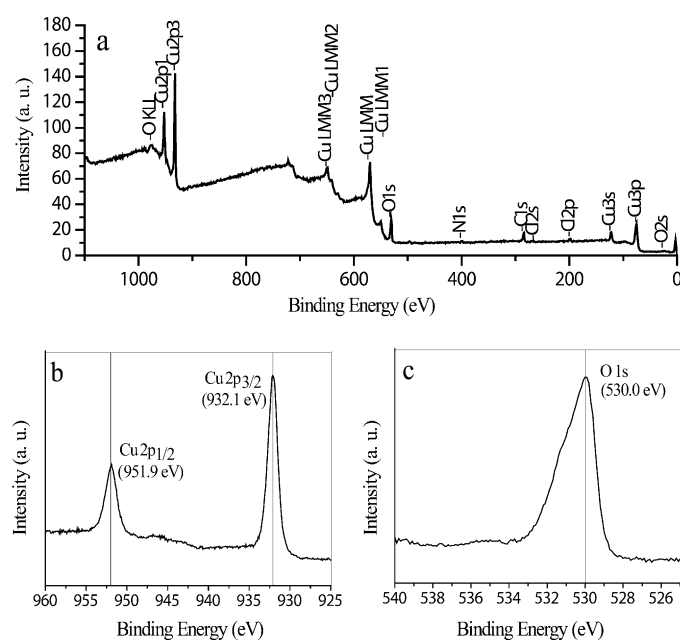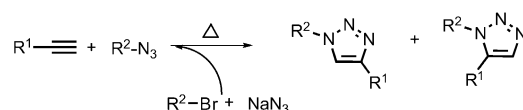
Figure 2. a) XPS spectrum of rhombic dodecahedral $Cu_2O$ nanocrystals. b, c) Magnified XPS spectra showing the exact positions of the Cu 2p and O 1s peaks.



Scheme 1. A typical click reaction involves first the preparation of an alkyl or aromatic azide, followed by its reaction with an alkyne to obtain the product. Depending on the reaction temperature, regioisomers can form.

tent with the $Cu^I$ oxidation state. The O 1s peak appearing at 530.0 eV is comparable with the literature value at 530.2 eV for $Cu_2O$.[25] Sulfonic acid has been reported to show O 1s peak at 531.7 eV.[26] Thus, the XPS results indicate that the oxygen peak comes from $Cu_2O$, not from oxygen atoms on SDS. The absence of surfactant on the surface of the nanocrystals was also confirmed by the absence of the $S 2p_{3/2}$ and $S 2p_{2/1}$ peaks at 167.8 and 168.9 eV, respectively, from the sulfate species of SDS.[24] The surfactant-free nanocrystals can be directly used for their catalytic activity comparison provided that the amounts of nanocrystal samples used have the same total surface area.[27] Specific surface areas of the nanocrystals were obtained from the nitrogen adsorption/ desorption curves and BET surface area calculations (Figure S5, the Supporting Information). $Cu_2O$ nanocubes, octahedra, and rhombic dodecahedra weighing 22.4, 25.1, 23.0 mg, respectively, were used for the surface area measurements. The surface areas of $Cu_2O$ nanocubes, octahedra, rhombic dodecahedra, and commercially available $Cu_2O$ powder from Aldrich were found to be 2.84, 0.56, 1.35, and 1.18 $m^2 g^{-1}$, respectively. From these numbers, 1 mg of nanocubes, 5 mg of octahedra, and 2 mg of rhombic dodecahedra

with a calculated total particle surface area of $\approx 0.0028$ $m^2 g^{-1}$ were used for all the catalytic reactions in this study. Please note that the conventional practice of loading amount and mole percent of catalyst is not suitable for this study, because the total surface area, rather than the weight of the catalyst, is more important for facet-dependent catalytic activity investigation.

For the [3+2] cycloaddition reactions by click chemistry, azides are typically obtained from the reaction of organic halides and $NaN_3$. The synthesized azides subsequently react with aliphatic or aromatic alkynes to give the final products (see Scheme 1). Such an approach has been adopted for most nanoparticle-catalyzed click reactions.[20a,b,22] In this work, we found that a one-pot multicomponent click reaction can be successfully carried out using the $Cu_2O$ nanocrystal catalysts, thus a single reaction directly gives the cycloaddition product. For the initial reaction, benzyl bromide and $NaN_3$ were subjected to a [3+2] cycloaddition reaction with phenyl acetylene for the one-pot synthesis of 1-benzyl-4-phenyl-1$H$-1,2,3-triazole in ethanol at 55 °C under nitrogen atmosphere (see Table 1). Upon completion of the reaction, the $^1H$ NMR spectra of the as-synthesized product indicate

Table 1. Comparison of the catalytic activity of different $Cu_2O$ nanocrystals for different 1,3-dipolar cycloaddition reactions.[a]



| Alkynes | Organic halides | Product | $t$ [h] | RD Yield [%][b] | $t$ [h] | OC Yield [%][b] | $t$ [h] | Cube Yield [%][b] |
|---|---|---|---|---|---|---|---|---|
| 1 **1a** | **2a** Br | **3a** | 1 | 96 | 4.5 | 90 | 7 | 88 |
| 2 **1c** | **2a** Br | **3c** | 1.5 | 92 | 5 | 88 | 7 | 80 |
| 3 **1b** OH | **2c** Br | **3n** OH | 2 | 90 | 5.5 | 90 | 8 | 77 |

[a] Reagents and conditions: **1** (0.25 mmol), **2** (0.25 mmol), and $NaN_3$ (0.38 mmol) in EtOH (3 mL) at 55 °C. RD = rhombic dodecahedra; OC = octahedra. [b] Yield of the isolated product.

regioselective formation of pure 1,4-disubstituted triazoles without any by-products. $Cu_2O$ nanocubes gave a yield of 88 % after 7 h of reaction, whereas octahedra delivered a 90 % yield in 4.5 h. Therefore, octahedra are catalytically more efficient than the nanocubes for this reaction. Remarkably, rhombic dodecahedra achieved a 96 % yield after

just 1 h of reaction. Rhombic dodecahedra are clearly the best and most efficient catalysts among these three nanocrystal morphologies. By comparison, the commercially available $Cu_2O$ powder with larger grain sizes showed 80% yield in 5 h (see Table S2, the Supporting Information). Turnover frequencies (TOF) have been determined for these three particle shapes. TOF numbers for the $Cu_2O$ nanocubes, octahedra, and rhombic dodecahedra are 616, 754, and 6652 $h^{-1}$, respectively, again showing the rhombic dodecahedra as highly efficient catalysts (see the Supporting Information for the calculations). To show the rhombic dodecahedra as consistently the best catalysts, two more reactions using quite different alkynes and organic halides as reagents were performed (entries 2 and 3, Table 1). Again rhombic dodecahedra achieved high yields in substantially less time than the nanocubes and octahedra, and are the best catalysts for a broad range of click reactions. Since the reaction takes place on the particle surfaces, the catalytic activity differences are ascribed to the different facets exposed (i.e., {110} > {111} > {100}).

To confirm that the observed catalytic activity of $Cu_2O$ nanocrystals is not due to dissolved $Cu^I$ species in the solution, control experiments were performed. First, we took 3 mg of $Cu_2O$ rhombic dodecahedra in ethanol and stirred the particles for 2.5 h under a nitrogen atmosphere at 55°C to simulate the actual conditions used for the click reactions. After centrifugation at 5000 rpm for 3 min, the supernatant liquid was carefully collected. Using the supernatant liquid, click reaction was performed under the same reaction condition as stated in the experimental section. After 8 h, we did not obtain any trace of click product from the reaction mixture, indicating the absence of $Cu^+$ ions in the supernatant liquid. Furthermore, solutions of CuCl and $CuCl_2$ in ethanol were prepared and their UV/Vis spectra were taken. Concentrated HCl was added to the CuCl solution to improve CuCl solubility. To the supernatant liquid, 0.1 M NaCl and 20 μL of concentrated HCl were added to test the presence of any copper species by forming CuCl or $CuCl_2$. The UV/Vis spectrum of the resulting supernatant liquid did not show any peak in the 200–800 nm range, but several absorption bands were recorded for CuCl and $CuCl_2$ in this spectral range (Figure S6, the Supporting Information). The results further verify the absence of dissolved $Cu^I$ species in the solution, and the observed catalytic activity is attributed to the catalytic action of the $Cu_2O$ nanocrystals.

Next, the effect of solvents on the coupling reaction was investigated using rhombic dodecahedra as the catalysts (Table S3, the Supporting Information). When the reactions were conducted in EtOH, EtOH/$H_2O$ (1:1 volume ratio), and $H_2O$, the products were obtained in excellent yields (92–96%). The use of $CH_3CN$ and THF as solvent did not yield the desired product. SEM images of $Cu_2O$ rhombic dodecahedra after 1.5 h of reaction in THF show the particles are coated with a thick layer of substance, thus blocking the catalytic sites (Figure S7, the Supporting Information). When $CH_3CN$ was used as the solvent, the particles were observed to be highly etched possible due to the coordina-

tion of $CH_3CN$ to the surface copper atoms.[28] The results show that the click reactions can be carried out in green solvents. Interestingly, around 20% of the rhombic dodecahedra became slightly etched during reaction in water, so ethanol is a better solvent to use. Since the solution pH is nearly neutral, dissolved oxygen may be a possible source of etchant in water.

The recyclability of the $Cu_2O$ rhombic dodecahedra was also examined. After finishing one run of the reaction, another cycle of the reaction was carried out using the same nanocrystals. It has been observed that the rhombic dodecahedra are effective and recyclable catalysts for 1,3-dipolar cycloaddition leading to the regioselective synthesis of 1,4-disubstituted triazole (**3a**) with excellent product yields of 92–96% after 1 h of reaction in the second cycle. SEM images of the $Cu_2O$ rhombic dodecahedra after completing two cycles of 1,3-dipolar cycloaddition reaction show no noticeable changes in morphology, supporting their use as recyclable catalysts (Figure 3).
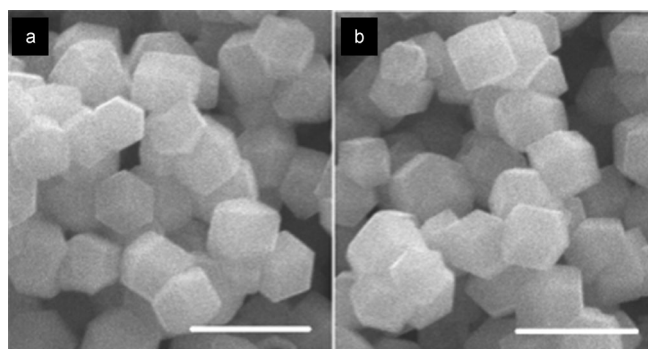


Figure 3. SEM images of the rhombic dodecahedral $Cu_2O$ nanocrystals a) before and b) after two cycles of 1,3-dipolar cycloaddition reaction. Scale bar is equal to 500 nm.

A simple analysis of the different crystal planes of $Cu_2O$ can assist the explanation of the experimental observations. Figure 4 presents crystal models of the (100), (110), and (111) planes of $Cu_2O$. The (100) planes comprise the surface planes of a body-centered cubic unit cell of $Cu_2O$ with oxygen atoms forming the crystal lattice and copper atoms occupying half of the tetrahedral sites.[9] However, the (100) plane can also be presented to expose terminal Cu atoms.[29] For consistency with experimental observations of the low reactivity of nanocubes, the surface Cu atoms are considered to lie just below the uppermost layer of oxygen atoms. The (111) plane contains terminal copper and oxygen atoms. However, many of the surface Cu atoms reside below the plane of surface oxygen atoms (see Figure 4c).[30] The (110) plane is terminated with copper and oxygen atoms lying essentially on the same plane, and so all the surface Cu atoms are fully exposed (see Figure 4f). An area density analysis of surface Cu atoms reveals that the (110) plane actually has the lowest surface Cu atom density (10.98, 14.27, and 7.76 Cu atoms $nm^{-2}$ for the (100), (111), and (110) planes of
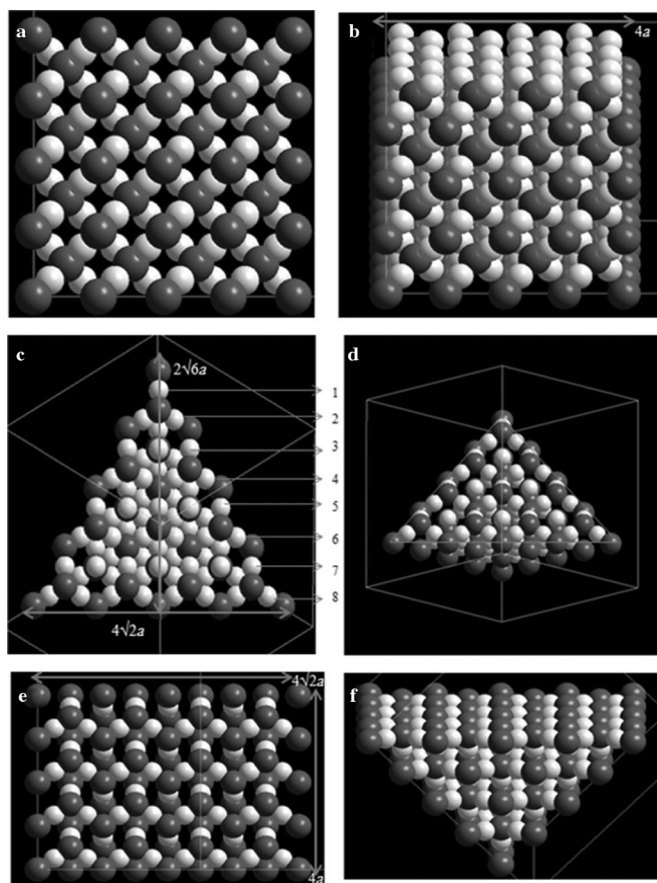
Figure 4. Crystal structure models of cuprite $Cu_2O$ showing the a, b) {100}, c, d) {111}, and e, f) {110} surfaces. Oxygen atoms are shown in a dark color, whereas copper atoms are shown in white. Two different viewing angles have been presented for each surface to more clearly show the number of surface atoms. For panel (b), the uppermost layer of oxygen atoms have been removed to clearly show the number of surface copper atoms. Panel (d) shows the {111} planes rotated 63° with respect to the model shown in panel (c). The triangle in panel (d) encloses the same area as that shown in panel (c). The cubic unit cell parameter is a.
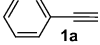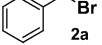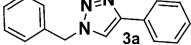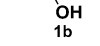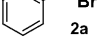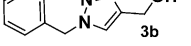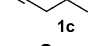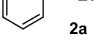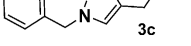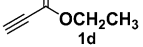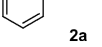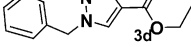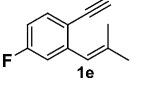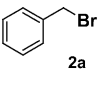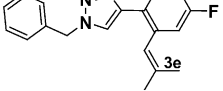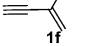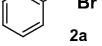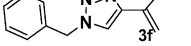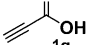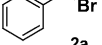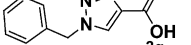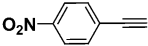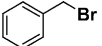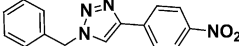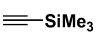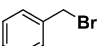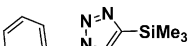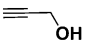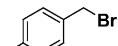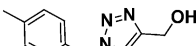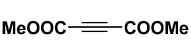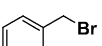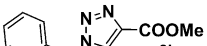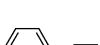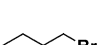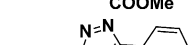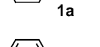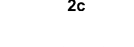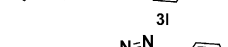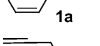
$Cu_2O$, respectively). However, all of the surface Cu atoms on the (110) planes are fully exposed for interaction with ligands, whereas many of the surface Cu atoms are partially blocked for the (111) planes and only partially exposed Cu atoms are available for the (100) plane to hinder the ligand interaction. These differences explain the observed relative catalytic activity of these surfaces. It is known that the first step of the [3+2] cycloaddition reaction involves the formation of Cu-acetylide through the cationic displacement of terminal protons of alkynes by the positively charged Cu atoms (Scheme S1, the Supporting Information).[31] The formation of Cu-acetylide happens on the $Cu_2O$ nanocrystal surface. Mixing terminal alkynes with $Cu_2O$ rhombic dodecahedra immediately form Cu-acetylide because of the fully exposed Cu atoms on the (110) planes, which reacts with in situ-generated azides to form 1,4-disubstituted triazoles in a short time. To further substantiate the greater catalytic activity of the {110} faces, ζ potential measurements on the freshly prepared $Cu_2O$ nanocrystals in pure methanol solu-

tion were carried out (Figure S8, the Supporting Information). The measured ζ potentials for $Cu_2O$ nanocubes, octahedra, and rhombic dodecahedra are +0.37, +6.9, and +14.5 mV respectively, which agree well with the crystal plane analysis. The surface charge of $Cu_2O$ nanocubes is close to neutral, whereas the positive surface charge of rhombic dodecahedra is 2.1 times higher than octahedra. The higher adsorption capability of anionic deprotonated alkynes on the positively charged and more accessible Cu atoms of $Cu_2O$ should favor the formation of the Cu-acetylide active species and increase the reaction rate. Thus, $Cu_2O$ rhombic dodecahedra with the fully exposed terminal Cu atoms show the best catalytic activity.

$Cu_2O$ rhombic dodecahedra have been subsequently employed as catalysts to a wide variety of terminal alkynes and organic halides using the optimized reaction conditions and the results are summarized in Table 2. The corresponding 1,4-disubstituted triazoles were obtained as highly regioselective products with excellent yields after a simple work-up involving centrifugation to remove the nanocrystals, washing and solvent evaporation. Finally the crude products were purified by column chromatography followed by spectroscopic characterization using $^1H/^{13}C$ NMR spectroscopy, and high-resolution mass spectroscopy (HR-MS). Substituent effects of both azide precursors and alkynes have be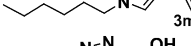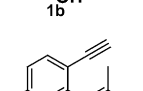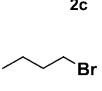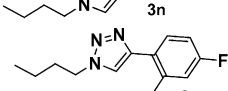en observed. The use of benzyl bromides or substituted benzyl bromides containing electron donating groups reacted nicely to obtain the corresponding triazoles in excellent yields (entries 1–11, Table 2). Interestingly, deactivated halides such as n-butyl bromides and n-hexyl bromides reacted with terminal alkynes in 1.5–2 h to obtain the 1,4-disubstituted triazoles in excellent yields (entries 12–15, Table 2). Apart from organic halides, it has been observed that aromatic alkynes containing electron-withdrawing groups such as $NO_2$, F, or sterically hindered substituents have no effect on the outcome of the reaction (entries 5, 8, and 15, Table 2). Hydroxy-substituted alkynes such as propargyl alcohol reacted nicely with both activated and unactivated organic halides to obtain the corresponding triazoles as single regioisomers in good to high yields (entries 2, 10, and 14, Table 2). Furthermore, alkynes bearing electron-withdrawing substituents such as ethyl propiolate and propiolic acid underwent triazole-forming reactions with high yields (entries 4 and 7, Table 2) compared with the slugging nature of the aliphatic alkynes (entry 3, Table 2). In addition, disubstituted acetylenes such as dimethylacetylene dicarboxylate (DMAD) reacted with benzyl bromides and $NaN_3$ under these optimized reaction conditions to obtain the 1,4-disubstituted triazoles in excellent yields (entry 11, Table 2).

After the successful regioselective syntheses of a wide variety of 1,4-disubstituted triazoles, we considered the synthesis of rufinamide (**A**), an antiepileptic drug, through this multicomponent coupling reaction. This drug is usually prepared by multistep procedures, and its synthesis requires the use of a high temperature (135 °C) and long reaction times (more than 1 day).[32] The synthetic conditions are time- and energy-consuming. We recognized that rufinamide (**A**)

Table 2. A list of three-component 1,3-dipolar cycloaddition reactions catalyzed by Cu$_2$O rhombic dodecahedra using organic halides, alkynes, and NaN$_3$.[a]

$$R^1\text{—}\equiv \;+\; NaN_3 \;+\; R^2\text{-Br} \xrightarrow[\text{55 °C, EtOH, under N}_2\text{ atm}]{\text{Cu}_2\text{O rhombic dodecahedra}} \; 3$$



| | Alkynes | Organic halides | Product | Mass | t [h] | Yield [%][b] |
|---|---|---|---|---|---|---|
| 1 | 1a | 2a | 3a | 235 | 1 | 96 |
| 2 | 1b | 2a | 3b | 189 | 1 | 93 |
| 3 | 1c | 2a | 3c | 201 | 1.5 | 92 |
| 4 | 1d | 2a | 3d | 231 | 1 | 89 |
| 5 | 1e | 2a | 3e | 307 | 2.5 | 91 |
| 6 | 1f | 2a | 3f | 199 | 1.5 | 93 |
| 7 | 1g | 2a | 3g | 203 | 1 | 98 |
| 8 | 1h | 2a | 3h | 280 | 1 | 90 |
| 9 | 1i | 2a | 3i | 231 | 1 | 92 |
| 10 | 1b | 2b | 3j | 203 | 1 | 94 |
| 11 | 1j | 2a | 3k | 275 | 1 | 97 |
| 12 | 1a | 2c | 3l | 201 | 1.5 | 91 |
| 13 | 1a | 2d | 3m | 229 | 1.5 | 94 |
| 14 | 1b | 2c | 3n | 155 | 2 | 90 |
| 15 | 1e | 2c | 3o | 273 | 2 | 92 |

[a] Reagents and conditions: **1** (0.25 mmol), **2** (0.25 mmol), and NaN$_3$ (0.38 mmol) in EtOH (3 mL) at 55 °C. [b] Yield of the isolated product.

## Conclusion

We have employed surfactant-free Cu$_2$O nanocubes, octahedra, and rhombic dodecahedra as catalysts for the multicomponent synthesis of 1,2,3-triazoles in ethanol by 1,3-dipolar cycloaddition reactions. All these nanocrystals can serve as efficient catalysts for the one-pot click reactions. However, the Cu$_2$O rhombic dodecahedra bounded by the {110} facets are the best catalysts with the highest yields and shortest reaction times for a broad range of reagents used. They have also been demonstrated to be highly efficient for the one-pot synthesis of rufinamide. The Cu$_2$O rhombic dodecahedra are promising efficient and green heterogeneous catalysts for other types of coupling reactions.

## Experimental Section

**Chemicals**: Anhydrous copper(II) chloride (CuCl$_2$; 97%) and hydroxylamine hydrochloride (NH$_2$OH·HCl; 99%) were purchased from Aldrich. Sodium hydroxide (98.2%) and sodium dodecyl sulfate (SDS; 100%) were acquired from Mallinckrodt. All chemicals were used as received without further purification along with deionized water for all solution preparations. Commercially available reagents were used for the 1,3-dipolar cycloaddition reactions.

**Synthesis of Cu$_2$O nanocubes and rhombic dodecahedra**: The synthetic method described here is adopted from our previously reported procedure.[2] For the synthesis of Cu$_2$O nanocrystals with cubic and rhombic dodecahedral shapes, 8.92 and 6.95 mL of deionized water were added in turn

could be synthesized through a multicomponent coupling reaction by employing 2,6-difluorobenzyl bromide (**2e**), NaN$_3$, and propiolamide (**1k**) (Scheme 2). Cu$_2$O rhombic dodecahedra were selected as the catalysts. Gratifyingly, this multicomponent cycloaddition reaction produced rufinamide (**A**) in 2.5 h at 55 °C with 95% yield. The huge advantage of using these nanocrystal catalysts for this important reaction is demonstrated.



Scheme 2. One-pot synthesis of rufinamide (**A**). RD = rhombic dodecahedra.

to sample vials. The volume of water added to each vials was adjusted in such a manner that after the addition of NH$_2$OH·HCl, the total volume of the final solution is 10 mL. The sample vials were placed in a water bath set at 30–32 °C. Then, a solution of CuCl$_2$ (0.1 M, 0.5 mL) and SDS powder (0.087 g) were added to the vials with vigorous stirring. When the solution became clear, a solution of NaOH (1.0 M, 0.18 mL) was added and shaken for ≈10 s. The solution turned light-blue immediately, due to the formation of threadlike Cu(OH)$_2$ precipitate. Finally, 0.40 and 2.37 mL of 0.1 M NH$_2$OH·HCl were quickly injected in 5 s for the synthesis of nanocubes and rhombic dodecahedra, respectively. After stirring for 20 s, the solutions were kept in the water bath for 1 h for nanocrystal growth. The concentrations of Cu$^{2+}$ ions and SDS surfactant in the final solution are $1.0 \times 10^{-3}$ and $3.0 \times 10^{-2}$ M, respectively. The reaction mixtures were centrifuged at 5000 rpm for 3 min. After decanting the top solution, the precipitate was washed with 6 mL of 1:1 volume ratio of water and ethanol for three times to remove unreacted chemicals and SDS surfactant. The final washing step used 5 mL of ethanol, and the precipitate was dispersed in 0.6 mL of ethanol for storage and analysis.

**Synthesis of Cu$_2$O octahedra**: The synthetic procedure used for making octahedral Cu$_2$O nanocrystals is based on our reported procedure with a slight modification in the volume of NH$_2$OH·HCl solution added.[3] First, deionized water (9.02 mL) was added to a sample vial. The sample vial was placed in a water bath set at 30–32 °C. Next, CuCl$_2$ (0.1 mL of 0.1 M) and a solution of NaOH (0.2 mL, 1.0 M) were added and the vial was shaken for ≈10 s. Then, SDS powder (0.087 g) was introduced with vigorous stirring. Finally, NH$_2$OH·HCl (0.68 mL, 0.2 M) was quickly injected. After stirring for 20 s, the solution was kept in the water bath for 2 h for nanocrystal growth. The concentrations of Cu$^{2+}$ ions and SDS surfactant in the final solution are $1.0 \times 10^{-3}$ and $3.0 \times 10^{-2}$ M. The reaction mixture was centrifuged at 3500 rpm for 2 min. After decanting the top solution, the precipitate was washed with 6 mL of 1:1 volume ratio of water and ethanol for three times to remove unreacted chemicals and SDS surfactant. The final washing step used 5 mL of ethanol, and the precipitate was dispersed in ethanol (0.6 mL) for storage and analysis.

**Cu$_2$O nanocrystal-catalyzed click reactions**: Under an atmosphere of N$_2$ gas, a 25 mL round-bottomed flask containing a stirrer bar was charged with benzyl bromide (0.0428 g, 0.25 mmol, 1.0 equiv) and NaN$_3$ (0.026 g, 0.40 mmol, 1.6 equiv) in ethanol (5 mL). After the mixture was stirred for 10 min at room temperature, phenyl acetylene (0.0255 g, 0.25 mmol, 1.0 equiv) was added into the solution. A fixed amount of Cu$_2$O nanocrystals was immediately added to the reaction mixture (1 mg of nanocubes, 5 mg of octahedra, or 2 mg of rhombic dodecahedra with a calculated total particle surface area of 0.0028 m$^2$ g$^{-1}$). Subsequently, the reaction mixture was heated to 55 °C with stirring. The progress of the reaction was monitored by thin-layer chromatography (TLC). After completion, the reaction mixture was centrifuged at 5000 rpm for 3 min to remove the nanocrystals. The solvent was then removed under reduced pressure. Water (5 mL) was added to the resulting mixture, followed by extraction with ethyl acetate (10 mL twice). The combined organic layer was dried over anhydrous MgSO$_4$. The combined filtrate was subjected to evaporation to obtain the crude compound, which was purified over silica gel column (60–120 mesh) using 1% ethyl acetate in hexane as eluent to obtain the corresponding triazole as the product. To evaluate the extent of versatility of these nanocrystal catalysts, the same cycloaddition reaction was repeated with different substituents on organic halides and alkynes containing electron-donating and electron-withdrawing groups. Cu$_2$O rhombic dodecahedra were chosen as the catalysts in these reactions.

**Recyclability of the Cu$_2$O rhombic dodecahedra for the click reactions**: The recyclability of the Cu$_2$O rhombic dodecahedra as catalysts was also surveyed. After completing one run of the reaction, the reaction mixture was centrifuged. The solution containing the product was removed, leaving behind the nanocrystal precipitate. To the freshly taken ethanol solution, freshly measured quantities of benzyl bromide and NaN$_3$ were added. After stirring for 10 min, phenyl acetylene and the used nanocrystals were added into the solution. Subsequently, the reaction mixtures were heated to 55 °C with stirring. The progress of the reaction was also monitored by TLC.

**Instrumentation**: SEM images of the samples were obtained using a JEOL JSM-7000F electron microscope. XRD patterns were recorded on a Shimadzu XRD-6000 diffractometer with Cu$_{K\alpha}$ radiation. One drop of the Cu$_2$O nanocrystal solution was added to an optical microscope cover slide and dried naturally. The slide was mounted onto a sample holder for the XRD measurements. FT-IR spectra were taken on a Perkin–Elmer 55855 spectrometer. XPS characterization was carried out on a ULVAC-PHI Quantera SXM high-resolution XPS spectrometer. Data were recorded using a monochromatized Al anode as the excitation source. The C1s peak was chosen as the reference line. Surface areas of the three samples of Cu$_2$O nanocrystals were determined through nitrogen adsorption–desorption isotherms at 77 K using a Quantachrome Nova 2000e analyzer. $\zeta$ potential measurements were carried out on a Malvern particle size analyzer MS2000. $^1$H NMR (600 MHz) and $^{13}$C NMR (150 MHz) spectra were recorded with a Bruker DRX600 spectrometer. Chemical shifts are reported in ppm relative to the internal solvent peak ($\delta = 7.24$ and 77.0 ppm, respectively, for CDCl$_3$). Coupling constants, $J$, are given in Hz. Multiplicities of peaks are given as d (doublet), m (multiplet), s (singlet), and t (triplet). TLC plates were Merck silica gel 60 F254 on aluminum. Flash column chromatography was performed with silica gel (60–100 mesh). All reagents required for the 1,3-dipolar cycloaddition reactions are available commercially.

[1] C. H. Kuo, M. H. Huang, *Nano Today* **2010**, *5*, 106–116.
[2] W.-C. Huang, L.-M. Lyu, Y.-C. Yang, M. H. Huang, *J. Am. Chem. Soc.* **2012**, *134*, 1261–1267.
[3] J.-Y. Ho, M. H. Huang, *J. Phys. Chem. C* **2009**, *113*, 14159–14164.
[4] X. Wang, H. F. Wu, Q. Kuang, R. B. Huang, Z. X. Xie, L. S. Zheng, *Langmuir* **2010**, *26*, 2774–2778.
[5] L.-M. Lyu, W.-C. Wang, M. H. Huang, *Chem. Eur. J.* **2010**, *16*, 14167–14174.
[6] P. Yang, *Nature* **2012**, *482*, 41–42.
[7] M. H. Huang, P.-H. Lin, *Adv. Funct. Mater.* **2012**, *22*, 14–24.
[8] C.-H. Kuo, M. H. Huang, *J. Phys. Chem. C* **2008**, *112*, 18355–18360.
[9] Y. Zhang, B. Deng, T. Zhang, D. Gao, A. W. Xu, *J. Phys. Chem. C* **2010**, *114*, 5073–5079.
[10] C.-H. Kuo, Y.-C. Yang, S. Gwo, M. H. Huang, *J. Am. Chem. Soc.* **2011**, *133*, 1052–1057.
[11] W.-C. Wang, L.-M. Lyu, M. H. Huang, *Chem. Mater.* **2011**, *23*, 2677–2684.
[12] L.-M. Lyu, M. H. Huang, *J. Phys. Chem. C* **2011**, *115*, 17768–17773.
[13] C.-H. Kuo, M. H. Huang, *J. Am. Chem. Soc.* **2008**, *130*, 12815–12820.
[14] a) B. X. Tang, F. Wang, J. H. Li, Y. X. Xie, M. B. Zhang, *J. Org. Chem.* **2007**, *72*, 6294–6297; b) H. Cao, H. Jiang, G. Yuan, Z. Chen, C. Qi, H. Huang, *Chem. Eur. J.* **2010**, *16*, 10553–10559.
[15] L. Li, C. Nan, Q. Peng, Y. Li, *Chem. Eur. J.* **2012**, *18*, 10491–10496.
[16] Y. Xu, H. Wang, Y. Yu, L. Tian, W. Zhao, B. Zhang, *J. Phys. Chem. C* **2011**, *115*, 15288–15296.
[17] H. C. Kolb, M. G. Finn, K. B. Sharpless, *Angew. Chem.* **2001**, *113*, 2056–2075; *Angew. Chem. Int. Ed.* **2001**, *40*, 2004–2021.
[18] a) R. Huisgen, *Pure Appl. Chem.* **1989**, *61*, 613–628; b) C. W. Tornøe, C. Christensen, M. Meldal, *J. Org. Chem.* **2002**, *67*, 3057–3064; c) V. V. Rostovtsev, L. G. Green, V. V. Fokin, K. B. Sharpless, *Angew. Chem.* **2002**, *114*, 2708–2711; *Angew. Chem. Int. Ed.* **2002**, *41*, 2596–2599.
[19] a) K. B. Sharpless, H. C. Kolb, *Drug Discovery Today* **2003**, *8*, 1128–1137; b) M. Meldal, C. W. Tornøe, *Chem. Rev.* **2008**, *108*, 2952–

3015; c) C. O. Kappe, E. V. Eycken, *Chem. Soc. Rev.* **2010**, *39*, 1280–1290; d) R. A. Decréau, J. P. Collman, A. Hosseini, *Chem. Soc. Rev.* **2010**, *39*, 1291–1301.

[20] a) L. D. Pachón, J. H. van Maarseveen, G. Rothenberg, *Adv. Synth. Catal.* **2005**, *347*, 811–815; b) B. H. Lipshutz, B. R. Taft, *Angew. Chem.* **2006**, *118*, 8415–8418; *Angew. Chem. Int. Ed.* **2006**, *45*, 8235–8238; c) F. Alonso, Y. Moglie, G. Radivoy, M. Yus, *Adv. Synth. Catal.* **2010**, *352*, 3208–3214; d) T. Jin, M. Yan, Y. Yamamoto, *ChemCatChem* **2012**, *4*, 1217–1229.

[21] F. Bebensee, C. Bombis, S.-R. Vadapoo, J. R. Cramer, F. Besenbacher, K. V. Gothelf, T. R. Linderoth, *J. Am. Chem. Soc.* **2013**, *135*, 2136–2139.

[22] Z. Zhang, C. Dong, C. Yang, D. Hu, J. Long, L. Wang, H. Li, Y. Chen, D. Kong, *Adv. Synth. Catal.* **2010**, *352*, 1600–1604.

[23] Z. C. Orel, A. Anžlovar, G. Dražić, M. Žigon, *Cryst. Growth Des.* **2007**, *7*, 453–458.

[24] C.-H. Kuo, Y.-T. Chu, Y.-F. Song, M. H. Huang, *Adv. Funct. Mater.* **2011**, *21*, 792–797.

[25] M. C. Biesingera, L. W. M. Laua, A. R. Gersonb, R. S. C. Smart, *Appl. Surf. Sci.* **2010**, *257*, 887–898.

[26] S. B. Idage, S. Badrinarayanan, S. P. Vernekar, S. Sivaram, *Langmuir* **1996**, *12*, 1018–1022.

[27] C.-Y. Chiu, P.-J. Chung, K.-U. Lao, C.-W. Liao, M. H. Huang, *J. Phys. Chem. C* **2012**, *116*, 23757–23763.

[28] J. R. Black, W. Levason, M. Webster, *Acta Crystallogr. C* **1995**, *51*, 623–625.

[29] K. X. Yao, X. M. Yin, T. H. Wang, H. C. Zeng, *J. Am. Chem. Soc.* **2010**, *132*, 6131–6144.

[30] a) Q. Hua, D. Shang, W. Zhang, K. Chen, S. Chang, Y. Ma, Z. Jiang, J. Yang, W. Huang, *Langmuir* **2011**, *27*, 665–671; b) M. Leng, C. Yu, C. Wang, *CrystEngComm* **2012**, *14*, 8454–8461.

[31] a) C. Shao, X. Wang, J. Xu, J. Zhao, Q. Zhang, Y. Hu, *J. Org. Chem.* **2010**, *75*, 7002–7005; b) F. Himo, T. Lovell, R. Hilgraf, V. V. Rostovtsev, L. Noodleman, K. B. Sharpless, V. V. Fokin, *J. Am. Chem. Soc.* **2005**, *127*, 210–216.

[32] W. H. Mudd, E. P. Stevens, *Tetrahedron Lett.* **2010**, *51*, 3229–3231.